Journal of the Korean Chemical Society
2018, *Vol. 62, No. 2*
Printed in the Republic of Korea
https://doi.org/10.5012/jkcs.2018.62.2.118

Characterization of Hexagonal Tungsten Bronze Cs_xWO_3 Nanoparticles and Their Thin Films Prepared by Chemical Coprecipitation and Wet-Coating Methods

Jun Young Kwak[‡], Tai Kyung Hwang[†], Young Hee Jung[‡], Juyun Park[†], Yong-Cheol Kang[†], and Yeong Il Kim[†,*]

[†]*Department of Chemistry, Pukyong National University, Busan 48513, Korea.* [*]*E-mail: ykim@pknu.ac.kr*
[‡]*Research Laboratory, Adchro, Inc., Busan 48547, Korea.*

(Received January 11, 2018; Accepted January 27, 2018)

ABSTRACT. The hexagonal tungsten bronze Cs_xWO_3 nanoparticle was synthesized by a chemical coprecipitation method of ammonium tungstate and Cs_2CO_3 in acidic condition. This synthetic method for cesium tungsten bronze is reported for the first time as far as we know. The synthesized Cs_xWO_3 as precipitated showed a weak crystallinity of hexagonal unit cell with a crystallite size of about 4 nm without annealing. When the synthesized Cs_xWO_3 was annealed in N_2 atmosphere, the crystallinity and crystallite size systematically increased maintaining the typical hexagonal tungsten bronze structure as the annealing temperature increased. The analyzed Cs content in the bronze was about 0.3 vs W, which is very close to the theoretical maximum value, 1/3 in cesium tungsten bronze. According to XPS analysis, the reduced tungsten ions existed as both the forms of W^{5+} and W^{4+} and the contents systematically increased as the annealing temperature increased up to 800 °C. The Cs_xWO_3 thin films on PET substrate were also prepared by a wet-coating method using the ball-milled solution of the annealed Cs_xWO_3 nanoparticles at various temperatures. The near-infrared shielding property of these thin films increased systematically as the annealing temperature increased up to 800 °C as expected with the increased contents of reduced tungsten ions.

Key words: Hexagonal tungsten bronze, Cs_xWO_3, Coprecipitation, Near infrared shielding

INTRODUCTION

Tungsten trioxide is the typical well-known chromogenic material that can change its color from colorless transparent to deep blue electrochromically,[1] photochromically[2] and gasochromically[3] by the reduction of W^{6+}. The reduced tungsten oxide, WO_{3-x} can also absorb or reflect near-infrared (NIR) light strongly as well as visible light absorption by a polaronic absorption mechanism[4] or the localized surface plasmon resonance.[5] Although this NIR shielding property of WO_{3-x} is promising for the application to heat-insulating windows, it is limited by the low visible light transmittance. Takeda et al. reported that the hexagonal tungsten bronzes with alkaline metal ions such as Cs, Rb, Tl have much higher visible transparency and excellent NIR shielding property than WO_{3-x}.[6] Among these tungsten bronzes Cs_xWO_3 has been most practically used for solar shielding films of automotive and building windows.[7]

The most cost-effective method of preparing thin films on any kind of substrate for practical applications is wet-coating method without high-temperature thermal treatment using coating solution including well-dispersed functional materials. It is essential to prepare functional nanoparticles as smaller as possible for this coating method. There have been reported only two types of methods of preparing nanoparticles of cesium tungsten bronze Cs_xWO_3: one is a solid-state synthesis of direct heating the mixtures of Cs and W precursor compounds.[6,8] The other one is hydrothermal or solvothermal synthesis of the precursors solution.[9] Although the traditional solid state synthesis is very facile and simple, it usually gives large fused polycrystalline particles and long-time milling is necessary to break down into smaller particles and this energetic milling often changes their original properties. The hydrothermal and solvothermal methods are difficult for a large-scale synthesis because of the limited volume of container and it usually takes long synthetic time. In this study we report, for the first time as far as we know, a facile chemical coprecipitation method of preparing cesium tungsten bronze nanoparticles. The subsequent annealing effect of the prepared tungsten bronze nanoparticle was investigated. The thin films of Cs_xWO_3 were also prepared by wet-coating method using the well-dispersed Cs_xWO_3 solution and their NIR shielding properties are investigated.

EXPERIMENTAL

Preparation

The mixture of 20.413 g of ammonium tungstate (99.99%, Sigma-Aldrich) and 12.448 g of cesium carbonate (99%, Alfa-Aesar) with about 1:1 molar ratio of Cs/W was dissolved in 300 mL of H_2O with some tricarboxylic acid at 80 °C.

An appropriate amounts of concentrated nitric acid (70%) was slowly dropped into the mixture and the reaction mixture was kept at 80 °C for 1 h. The precipitate was filtered and washed with copious amounts of water several times and lastly ethanol. The Cs_xWO_3 powder was finally obtained after being dried in vacuum oven in room temperature. The annealing of Cs_xWO_3 was performed in a tube furnace under the flow of N_2. The temperature was increased at the rate of 10 °C/min and kept for 3 h at the target temperatures. In order to prepare the thin film of Cs_xWO_3 on polyethylene terephthalate (PET) film, 10.0 g of the synthesized Cs_xWO_3 was ball-milled in 10.0 mL of ethanol with 0.5 mm zirconia beads for 7 days. Cs_xWO_3 solution in ethanol became almost clear solution after ball-milling. This Cs_xWO_3 solution was bar-coated on PET substrate of 100 mm thickness using an auto-film applicator equipped with no. 6 Meyer bar in the rate of 20 mm/s. The cast film of Cs_xWO_3 was dried at room temperature in air.

Characterization

The X-ray diffraction (XRD) patterns were carried out on Phillips X'Pert-MPD diffractometer using Cu Kα radiation source at a scan rate of 0.02° s^{-1}. The morphologies of the sample powders and thin films were characterized by field-emission scanning electron microscope (FE-SEM, Jeol JEM-6700F). The nanoparticles of Cs_xWO_3 in the ball-milled solution was characterized with field-emission transmission electron microscope (FE-TEM, Jeol JEM-2100F). X-ray photoelectron spectroscopic (XPS) data were collected with ESCALab MKII spectrometer. XPS spectra were obtained using an Al Kα X-ray source (1486.6 eV) and a channeltron with an acceleration voltage of 2850 V. Survey XPS spectra were obtained by constant analyzer energy mode with a pass energy of 50 eV and a step size of 0.5 eV. High resolution XPS spectra were collected by a pass energy of 20 eV, scan step of 0.05 eV. The deconvolution process was performed with an XPSPEAK4.1 program. The background was chosen in the Shirley mode and the ratio of Lorenz/Gaussian was 30/70. An energy dispersive X-ray spectroscopy (EDS) combined on FE-SEM and XPS were employed for the approximate elemental analyses of W and Cs. The visible and near-infrared spectra of the Cs_xWO_3 films were measured with JASCO V-670 spectrophotometer to characterize the near-infrared shielding properties.

RESULTS AND DISCUSSION

The addition of nitric acid into the mixture solution of polytungstate and cesium ion gave an immediate precipitation.

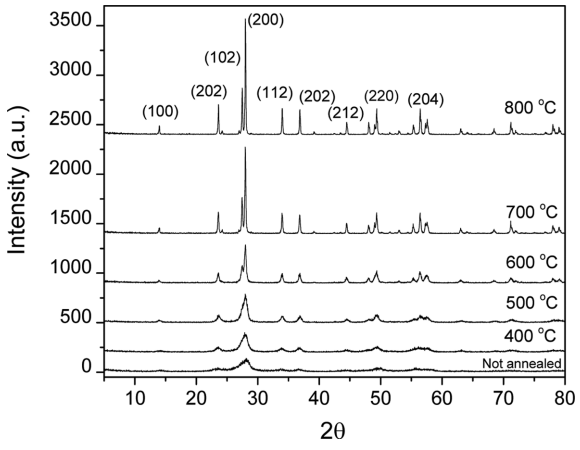

***Figure* 1.** XRD patterns of the Cs_xWO_3 samples that were annealed at the various temperatures in N_2 atmosphere.

The synthesis of WO_3 nanoparticles by the hydrolysis of tungstate in acidic medium has been known[10] but the synthesis of alkaline tungsten bronze by the acidic hydrolysis of tungstate has not been reported as far as we know. Since the theoretical maximum ratio of Cs/W is 1/3 in cesium tungsten bronze,[11] we used excess cesium ions by keeping the Cs/W ratio as about 1. *Fig.* 1 shows the XRD patterns of the prepared Cs_xWO_3 powder samples that was as precipitated and annealed in N_2 atmosphere at various temperatures. All the samples show the hexagonal crystal structure of the well-known tungsten bronze.[12] The sample as precipitated without annealing also show the weak crystallinity even though it was very poor. The crystallinity systematically increased as the annealing temperature increased. The crystallite sizes that were estimated by Scherrer equation using (200) peak were listed in *Table* 1.[13] The sizes were in the range of 4–70 nm depending on the annealing temperature and systematically increased as increasing the temperature. The crystallinity and size were changed largely at the temperatures in the range of 500–800 °C. The change was not very appreciable at the temperature higher than 800 °C,

***Table* 1.** The crystallite sizes and atomic ratios (Cs/W) of Cs_xWO_3 that were annealed at various temperatures in N_2 atmosphere, which is estimated from the XRD peak of (200) and EDS, respectively

Temperature (°C)	Crystallite Size (nm)	Cs/W
Not annealed	3.6	0.31
400	7.0	0.29
500	10.7	0.31
600	23.4	0.29
700	50.7	0.31
800	66.3	0.31

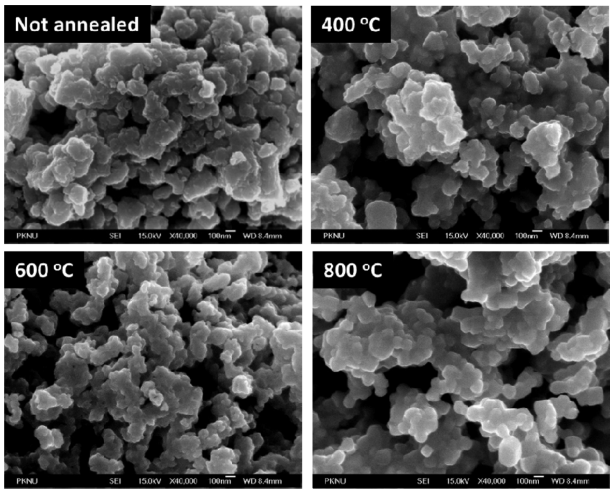

***Figure* 2.** FE-SEM images of Cs_xWO_3 powders that were annealed at the various temperatures.

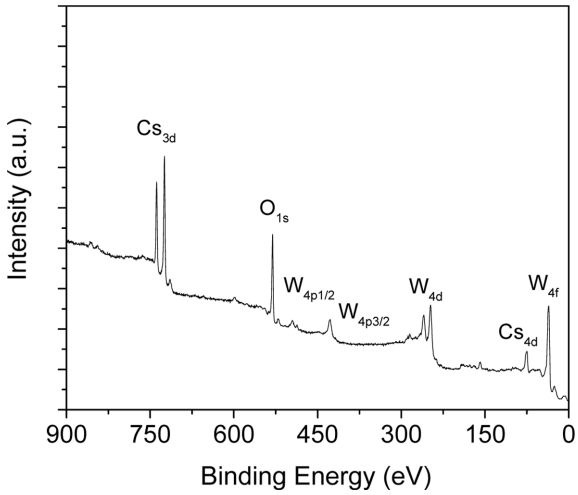

***Figure* 3.** XPS survey spectrum of Cs_xWO_3 samples that were annealed at 400 °C in N_2.

which was not shown here.

Fig. 2 shows the morphologies of Cs_xWO_3 powders that was as precipitated without annealing and annealed at various temperatures in N_2 atmosphere. The aggregated particles have the sizes of several hundred nm in all the cases and the morphologies were not much different irrespective of annealing temperatures up to 800 °C. This means that the annealing in N_2 did not seriously affect the fusion of crystalline particles in micrometer scale but it clearly influenced the crystallinity and crystalline size in nanometer scale as shown in *Fig.* 1 and *Table* 1. The cesium contents in the samples were analyzed with EDS. The data from three different sites for each sample were averaged and listed in *Table* 1. The atomic ratio of Cs/W was about 0.3 in all the samples, which is very close to the maximum value in hexagonal tungsten bronze structure of Cs_xWO_3. This ratio was approximately maintained if the ratio in the precursor solution was kept higher than 0.5. This EDS data confirmed the incorporation of cesium ion into WO_3 during the acid-precipitation of the tungstate by hydrolysis.

In order to study the oxidation states of W in Cs_xWO_3, we measured XPS data for the annealed samples. *Fig.* 3 shows the XPS survey spectrum of Cs_xWO_3 nanoparticles annealed at 400 °C in N_2. The peaks at binding energies corresponding to Cs, W and O were clearly seen. No extra element except carbon was detected. The atomic composition from the high resolution XPS spectra of Cs_{3d}, W_{4f} and O_{1s} was listed in *Table* 2. The atomic ratio of Cs/W was constant as about 0.22 irrespective of the annealing temperatures. According to Liu et al's study of Cs_xWO_3 that were prepared by a solvothermal method,[9d] the Cs/W ratio increased in the samples annealed at the higher temperature. Their explanation was that Cs^+ ion diffused out to the surface by the annealing. This phenomena didn't happen for our samples that were differently prepared by the acid coprecipitation. The value of CS/W ratio was lower than that from EDS data. That is obvious as expected because XPS data comes from only surface atoms whereas EDS, which is X-ray fluorescence, can measure a bulk average property. The high resolution XPS spectra of W_{4f} in the Cs_xWO_3 samples that were annealed at various temperatures were shown in *Fig.* 4(a). As the annealing temperature increased, the signal intensity and the splitting into $4f_{5/2}$ and $4f_{7/2}$ were decreased. The decreased intensity was due to the decreased powder density of lager

***Table* 2.** XPS analysis of Cs_xWO_3 samples that were annealed at the various temperatures

Annealing Temp. (°C)	Atomic Composition (%)				W composition (%)	
	Cs	W	O	Cs/W	W^{6+}	$W^{5+}+W^{4+}$
400	7.6	32.8	59.6	0.23	73.2	26.8
500	7.5	34.1	58.4	0.22	64.3	35.7
600	7.7	35.6	56.8	0.22	63.4	36.4
700	7.4	33.9	58.8	0.22	59.4	40.6
800	6.5	30.3	63.2	0.22	54.7	45.3

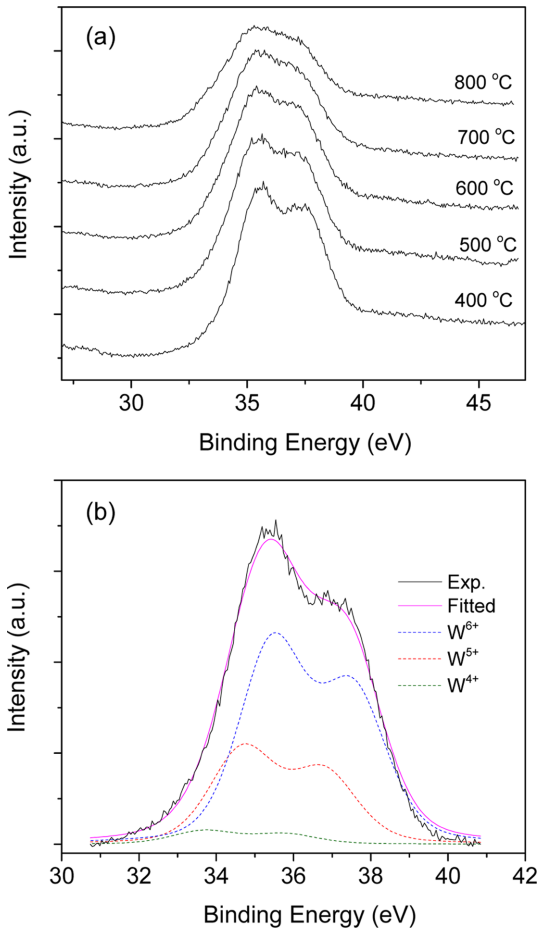

***Figure* 4.** (a) The high resolution XPS spectra of W_{4f} in Cs_x-WO_3 samples that were annealed at various temperatures and (b) the deconvoluted spectra of the sample that were annealed at 400 °C in N_2.

particles at the higher annealing temperature and the decreased slitting was due to the increased component of lower oxidation states. *Fig*. 4(b) shows the W_{4f} peak of the sample annealed at 400 °C that was deconvoluted into three oxidation states of W^{6+}, W^{5+} and W^{4+}. The deconvolution was not fitted well without W^{4+} component. The composition of W^{6+} and the reduced components (W^{5+}+W^{4+}) was listed in *Table* 2. As the temperature increased, the reduced tungsten ion components systematically increased as expected with the colors of the powders.

The thin films of Cs_xWO_3 that were annealed at the various temperatures were prepared on PET substrate by a wet-coating method. The coating solution was prepared by the ball-milling of Cs_xWO_3 powders in ethanol. The solution ball-milling is one of the common methods of dispersing the aggregated particles and making homogeneous suspension or clear solution without giving a strong stress.

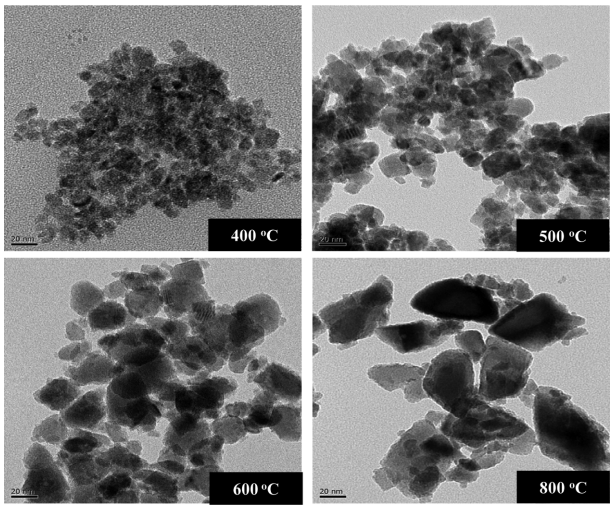

***Figure* 5.** FE-TEM images of Cs_xWO_3 nanoparticles that were annealed at various temperatures. The samples were obtained from the ball-milled coating solutions in ethanol.

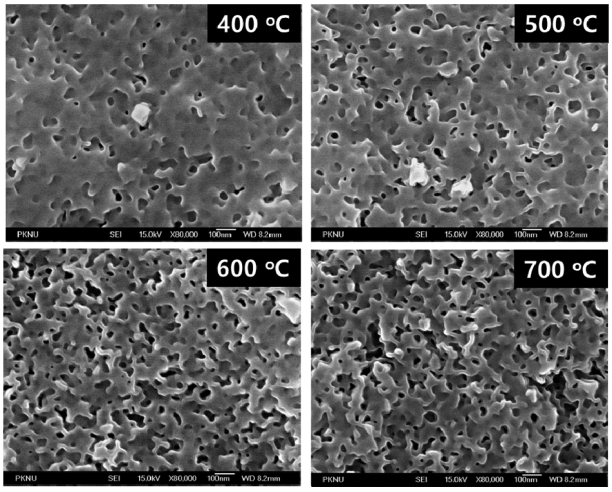

***Figure* 6.** FE-SEM images of Cs_xWO_3 films on PET substrate, of which Cs_xWO_3 samples were annealed at various temperatures.

Fig. 5 shows TEM images of Cs_xWO_3 nanoparticles, which were annealed at various temperatures, obtained from the ball-milled coating solution. After the ball-milling the aggregated particles that were shown in FE-SEM images of *Fig*. 2 were well dispersed and the individual crystalline particles were shown. The particle sizes systematically increased as the annealing temperature increased. The estimated sizes were in the range of 10–60 nm and pretty much matched with those estimated from XRD peaks mentioned above. The cast films prepared by a bar-coater from the coating solution without any polymer binder were very homogeneous and transparent with a thickness of about

150 nm. *Fig*. 6 shows FE-SEM images of Cs_xWO_3 films on PET substrate. The submicroscopic morphology of the films were nanoporous with the pores of less than 50 nm size for all the cases regardless of the annealing temperature. However, there was a slight difference for the surface roughness between the samples prepared at different annealing temperature. For the film prepared with the nanoparticles annealed at the higher temperature it had the more pores and the rougher the surface was as shown in the SEM images.

Fig. 7 shows the optical transmission spectra of Cs_xWO_3 thin films on PET substrate. The near-infrared transmittance of the films prepared with the annealed Cs_xWO_3 decreased as the annealing temperature increased. The decrease was almost linear until 600 °C. After 600 °C the decrease was not prominent and saturated above 800 °C. The NIR shielding effect of Cs_xWO_3 and WO_{3-x} is ascribed to the reduced tungsten ions whether it may be explained by a polaronic absorption mechanism or the localized surface plasmon resonance as mentioned in Introduction. Therefore our results of this NIR-shielding effect is consistent with XPS data that showed the increase of W^{5+} and W^{4+} in the samples with the increased temperatures. However, interestingly, this tendency is very different from the thin films of Cs_xWO_3 that were prepared by the solvothermal[9d], and hydrothermal[9g] methods. In both their cases, the best NIR shielding property was obtained from the sample that was annealed at the optimized temperature, which was 500 °C, much lower than 800 °C. Indeed, the samples annealed at 800 °C showed the very poor NIR absorption in their results. Their explanation for this optimized temperature is that the O/W atomic ratio

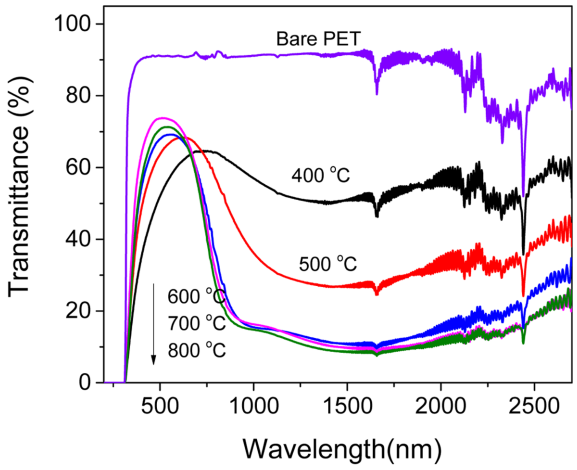

***Figure* 7.** Visible and NIR transmission spectra of the Cs_xWO_3 thin films on PET substrate, of which Cs_xWO_3 samples were annealed at various temperatures.

was minimized at 500 °C from XPS analysis and NIR-shielding was maximized due to the highest free carrier concentration for surface plasmon resonance. We doubt seriously their explanation because their XPS analysis showed that the ratio difference between 500 °C-annealed and 800 °C-annealed samples was only 0.08 and 700 °C-annealed sample, which had much better shielding property than 800 °C-sample, have the higher value than 800 °C-sample by 0.09. Considering the reliability of elemental analysis by XPS and their data fluctuation, their explanation cannot be acceptable at all.

CONCLUSION

We report for the first time the synthesis of Cs_xWO_3 nanoparticles that have a hexagonal tungsten bronze structure by a chemical coprecipitation method. The content of Cs in Cs_xWO_3 was about 0.3 vs W in atomic ratio, which is very close to the theoretical maximum value, 1/3 in hexagonal tungsten bronze structure. Although the Cs_xWO_3 nanoparticles as prepared have poor crystallinity with a size of ca. 4 nm in diameter, the annealing in N_2 atmosphere increased systematically the crystallinity and crystalline size as the temperature increased up to 800 °C. The annealing increased the ratio of reduced tungsten ions in both forms of W^{5+} and W^{4+} relative to W^{6+}. We have also prepared the Cs_xWO_3 thin films on PET substrate by a wet-coating method using the ball-milled solution of the Cs_xWO_3 nanoparticles annealed in N_2 at various temperatures. The near-infrared shielding property of these thin film systematically increased as the annealing temperature increased and it was almost saturated at 700 °C. This result was quite different from those of Cs_xWO_3 thin film that was prepared from the hydrothermal and solvothermal methods by Shi et al.[9g] and Liu et al.[9d], respectively.

Acknowledgments. This work was supported by a Research Grant of Pukyong National University (Year 2016).

REFERENCES

1. (a) Granqvist, C. G. *Electrochim. Acta* **1999**, *44*, 3005. (b) Granqvist, C. G. *Sol. Energy Mater. Sol. Cells* **2000**, *60*, 201.
2. Sun, M.; Xu, N.; Cao. Y. W.; Yao, J. M.; Wang, E. G. *J. Mater. Res.* **2000**, *15*, 927.
3. Schweiger, C.; Georg, A.; Graf, W.; Wittwer, V. *Sol. Energy Mater. Sol. Cells* **1998**, *54*, 99
4. Faughnan, B. H.; Crandall, R. S.; Heyman, P. M. *RCA Rev.* **1975**, *36*, 177.

5. Deneuville, A.; Gerard, P. *J. Electron. Mater.* **1978**, *7*, 559.
6. (a) Takeda, H.; Adachi, K. *J. Am. Ceram. Soc.* **2007**, *12*, 4059. (b) Yang, C.; Chen, J.-F.; Zeng, X.; Cheng, D.; Cao, D. *Ind. Eng. Chem. Res*. **2014**.
7. Machida, K.; Tofuku, A.; Adachi, K. *Handbook of Functional Nanomaterials*; Aliofkhazraei, M., Ed.; Nova Science Publishers: 2013; Vol. 1, pp 199-220.
8. (a) Zeng, X.; Zhou, Y.; Ji, S.; Luo, H.; Yao, H.; Huang, X.; Jin, P. *J. Mater. Chem. C* **2015**, *3*, 8050. (b) Lee, J.-S.; Liu, H.-C.; Peng, G.-D.; Tseng, Y. *J. Cryst. Growth* **2017**, *465*, 27.
9. (a) Liu, J. X.; Ando, Y.; Dong, X. L.; Shi, F.; Yin, S.; Adachi, K. *J. Solid State Chem.* **2010**, *183*, 2456. (b) Gao, C.; Yin, S.; Zhang, P.; Yan, M.; Adachi, K.; Chonan, T. Sato, T. *J. Mater. Chem.* **2010**, *20*, 8227. (c) Gao, C.; Yin, S.; Huang, L.; Yang, L.; Sato, T. *Chem. Comm.* **2011**, *47*, 8853. (d) Liu, J.-X.; Shi, F.; Dong, X.-L.; Yin, S.; Sato, T. *Mater. Character.* **2013**, *84*, 182. (e) Liu, J.; Xu, Q.; Shi, F.; Liu, S.; Luo, J.; Bao, L.; Feng, X. *App. Surf. Sci.* **2014**, *309*, 175. (f) Xu, Q.; Liu, J.; Shi, F.; Luo, J.; Jiang, Y.; Liu, G. *Adv. Mater. Res*. **2013**, *712-715*, 284. (g) Shi, F.; Liu, J.; Dong, X.; Xu, Q.; Luo, J.; Ma, H. *J. Mater. Sci. Technol.* **2014**, *30*, 342.
10. Supothina, S.; Seeharaj, P.; Yoriya, S.; Sriyudthsak, M. *Ceram. Int.* **2007**, *33*, 931.
11. Lee, K.-S.; Seo, D.-K.; Whangbo, M.-H. *J. Am. Chem. Soc.* **1997**, *119*, 4043.
12. JCPDS 83-1334.
13. Because the (102) and (200) peaks were overlapped in all the cases, two peaks of all the samples were deconvoluted into two Lorenzian peaks and the sizes were estimated with (200) peak.